

Giant $E1$ resonances in ${}^8\text{Be}$ from the reaction ${}^7\text{Li}(p, \gamma){}^8\text{Be}^\dagger$

G. A. Fisher,* P. Paul,† F. Riess,§ and S. S. Hanna

Department of Physics, Stanford University, Stanford, California 94305

(Received 21 January 1976)

The giant electric dipole resonances based on the ground state (0^+) and first excited state (2^+) of ${}^8\text{Be}$ have been studied with the reactions ${}^7\text{Li}(p, \gamma_0){}^8\text{Be}$ and ${}^7\text{Li}(p, \gamma_1){}^8\text{Be}$ over the range $E_p=0.8$ to 17.6 MeV. Both resonances show a simple resonant shape with little fine structure. The γ_1 giant resonance is displaced upward from the γ_0 resonance by an energy of 2.2 MeV which is approximately equal to the excitation of the 2^+ state. The reduced (γ, p_0) strengths of the two resonances are approximately equal and each exhausts about 10% of the $E1$ sum rule. The angular distributions for both γ_0 and γ_1 are quite constant over the giant resonance structure and are predominantly dipole in character. A simple model can be invoked to explain the dominant $E1$ features. The presence of $P_1(\cos\theta)$ and $P_3(\cos\theta)$ terms in both angular distributions indicates $E2$ strength which probably increases above the $E1$ resonances. Some parameters for the narrow levels at 18.15 and 19.06 MeV in ${}^8\text{Be}$ are given.

NUCLEAR REACTIONS ${}^7\text{Li}(p, \gamma)$, $E=0.8-17.6$ MeV; measured $\sigma(E; E_\gamma, \theta)$.
Deduced properties ${}^8\text{Be}$ levels at $E_x=18.15, 19.06$ MeV and γ_0, γ_1 giant resonances. 99% enriched ${}^7\text{Li}$ target.

I. INTRODUCTION

The giant electric dipole resonance (GDR) has been extensively studied throughout the nuclear table. It is generally characterized by a peak or peaks 3 to 5 MeV wide at an excitation energy that varies systematically from about 22 MeV in light nuclei to about 13 MeV in the heaviest nuclei.¹ Typically, the GDR exhausts the classical $E1$ sum rule.

In the $1p$ shell the GDR's have been studied extensively, with the experimental^{2,3} and theoretical^{4,5} emphasis on the $4N$ nuclei ${}^{16}\text{O}$ and ${}^{12}\text{C}$. As these nuclei correspond to closure of a major and a minor shell, respectively, the microscopic $1p-1h$ model^{6,7} has been applied to them and considerable success has been achieved in describing the basic features of their GDR's. It is the purpose of this work to study ${}^8\text{Be}$, the remaining $4N$ nucleus in this shell.^{8,9} Even though ${}^8\text{Be}$ is in the middle of a shell, one might expect its GDR to be similar to that of ${}^{12}\text{C}$, since all the particle-hole configurations in ${}^{12}\text{C}$ are available in ${}^8\text{Be}$ (see Table III). On the other hand, a tendency toward α clustering might produce an oblate shape in the ground state of ${}^{12}\text{C}$ and a prolate shape in that of ${}^8\text{Be}$. The influence of such ground state deformations on the shape of the GDR has been observed¹⁰ in heavy nuclei such as Ho and Ta and therefore might be present in ${}^8\text{Be}$. In addition, pronounced α clustering might make the GDR of ${}^8\text{Be}$ similar to that of ${}^4\text{He}$.

The (p, γ) reactions have proved invaluable in obtaining high-resolution, detailed information on the $E1$ giant resonances. Although the total photonuclear cross section (γ, tot) is of principal

interest, the basic features in the GDR are usually well reproduced in the (γ, p_0) channel. The (γ, p_0) yield can, of course, be obtained from the (p, γ_0) yield by detailed balance.

The (p, γ) reaction also can yield valuable information about photonuclear excitations built upon excited states. A study of the reaction ${}^7\text{Li}(p, \gamma_1){}^8\text{Be}(2.9)$ should be of interest since the first excited state of ${}^8\text{Be}$ might be described as the first excitation in a rotational band built upon the ground state. In this picture this state should have the same internal coordinates as the ground state and, therefore, the γ_0 and γ_1 giant resonances should be similar.

II. EXPERIMENTAL PROCEDURE

A monoenergetic proton beam was provided by the Stanford FN-tandem Van de Graaff accelerator; the resolution at 10 MeV was better than 5 keV. Thin targets of ${}^7\text{Li}$ were prepared by evaporating isotopically enriched (99%) metal samples in vacuum at the target site. The most successful targets were deposited on very thin (5 - 10 $\mu\text{g}/\text{cm}^2$) carbon foils. The proton beam passed through the target and backing and was stopped about 5 m downstream in a lead-lined and lead-shielded Faraday cup. At low incident energies, the proton beam could be stopped at or near the target by a thick tantalum disk without producing excessive background.

The energies of the capture gamma-rays observed in this experiment in the reaction ${}^7\text{Li}(p, \gamma){}^8\text{Be}$ lie in the range 18 to 33 MeV. In order to resolve the ground and first excited state transitions, a gamma ray spectrometer with a resolution

of 5% or better is desirable. The Stanford NaI spectrometer which has been described in detail elsewhere¹¹ was ideal for this study. Its salient features are its large size (24 cm \times 24 cm), an anti-pileup gate in the electronic circuit which suppresses the prolific low energy counting rate from the crystal, and a plastic scintillator which surrounds the main NaI crystal and is operated in anticoincidence with it.

An energy level diagram for ^8Be , showing the levels pertinent to this paper, is given in Fig. 1. A spectrum obtained from the NaI spectrometer for the reaction $^7\text{Li}(p,\gamma)^8\text{Be}$ is shown in Fig. 2, where the transitions to the ground state (γ_0) and the first excited state (γ_1) in ^8Be are readily apparent. Whereas the width of the γ_0 peak displays only the detector resolution, the γ_1 peak is clearly broadened by the 1.5-MeV width of the first excited state. The transition strengths to each state were obtained by fitting standard lineshapes to the data (see Fig. 2) by means of a chi-square com-

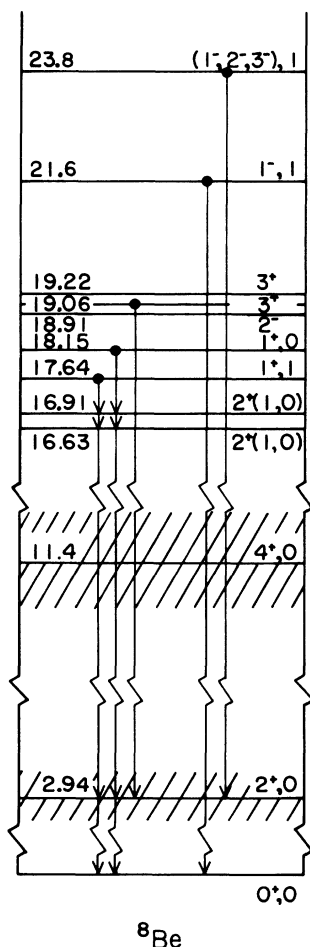


FIG. 1. Energy diagram of ^8Be indicating the levels of interest to radiative proton capture.

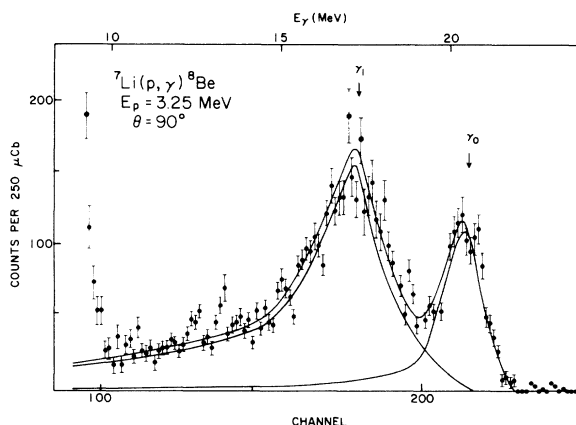


FIG. 2. Typical γ ray spectrum obtained with the large NaI detector equipped with anticoincidence shield. The transition to the ground state (γ_0) and the broadened first excited state (γ_1) are indicated along with typical fits using standard lineshapes.

puter program. The standard lineshape for the γ_0 transition was derived from the reaction $^{11}\text{B}(p,\gamma)^{12}\text{C}$. A broadened lineshape for the γ_1 transition was constructed by folding into the standard line a Lorentzian line with the width of the excited state. As a check on this procedure, the γ_1 lineshape was also obtained by subtracting the single line fit to γ_0 from a complete spectrum and using the remaining spectrum as the γ_1 lineshape to fit other spectra. The results obtained with both procedures agreed to within 5%. The tails of the gamma-ray lineshapes, obscured by background in the low-energy region, were extrapolated linearly to reach zero at zero energy ($E_\gamma = 0$). The systematic uncertainty introduced by this procedure is estimated to be approximately 10%.

III. RESULTS

Figure 3 displays the yields of γ_0 and γ_1 , obtained at 90° , over the range of excitation energies $E_x = 18$ MeV to 32.5 MeV. Both transitions exhibit a pronounced giant resonance with little additional structure except in the very low energy region.

Angular distributions of the γ yields were measured at energy intervals varying from 100 keV in the region of the main strength to 500 keV at higher energies. Figures 4 and 5 display representative angular distribution for γ_0 and γ_1 , respectively. The solid lines are least squares fits made to the data with the Legendre polynomial series

$$W(\theta) = A_0 \left[1 + \sum_{n=1}^N a_n P_n \right] \quad (1)$$

with $N = 2$. The total cross section

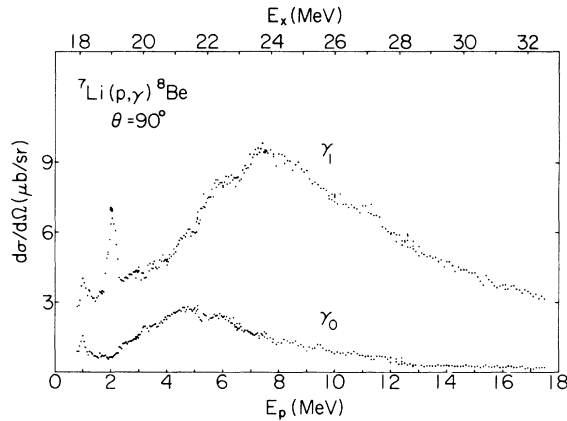


FIG. 3. The yield functions for the γ_0 and γ_1 transitions obtained at 90° , which show the broad giant resonances built on the ground state and the first excited state of ${}^8\text{Be}$.

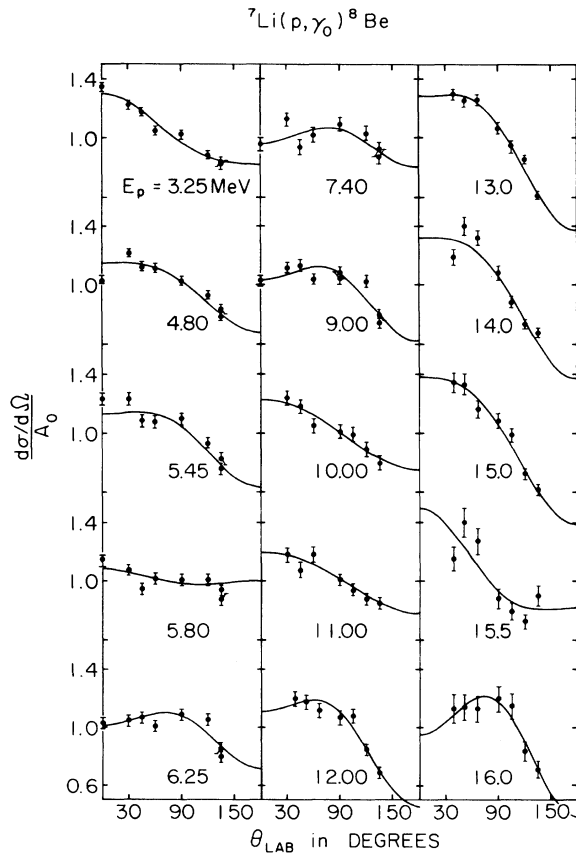


FIG. 4. Angular distributions obtained from the reaction ${}^7\text{Li}(p, \gamma_0){}^8\text{Be}$ over the energy range of the giant dipole resonance. The least-squares fits were computed with a series of Legendre polynomials up to $N = 2$.

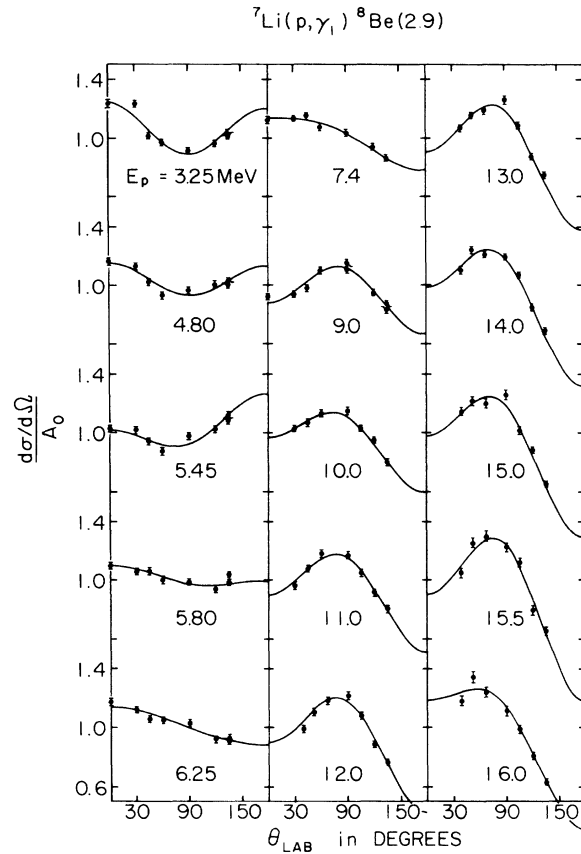


FIG. 5. Angular distributions obtained from the reaction ${}^7\text{Li}(p, \gamma_1){}^8\text{Be}$ over the energy range of the giant dipole resonance. The least-squares fits were computed with a series of Legendre polynomials up to $N = 2$.

$4\pi A_0$ and the normalized coefficients a_n which resulted from these fits and from more extensive fits with $N = 4$, are displayed in Figs. 6 and 7 for the γ_0 and γ_1 transitions, respectively. It appears that the fits are generally not improved in a statistically significant way by including coefficients higher than a_3 .

A. The low-lying resonances

Gamma decays from the three states in ${}^8\text{Be}$ at $E_x = 17.64$, 18.15 and 19.06 MeV (see Fig. 1) have previously been observed.^{12,13} Resonances corresponding to the latter two states can be clearly seen in Fig. 3 near $E_p = 1$ and 2 MeV. The state at 17.64 MeV was not studied in this work. The spectroscopic information derived from these measurements is compared to previous results in Table I.

The level at $E_x = 18.15$ MeV is known to have $J^\pi = 1^+$ and has established branches to the states at 0.0 , 2.9 , 16.6 and 16.9 MeV. Table I shows that the γ_1 width obtained here agrees well with previous observations, but the present γ_0

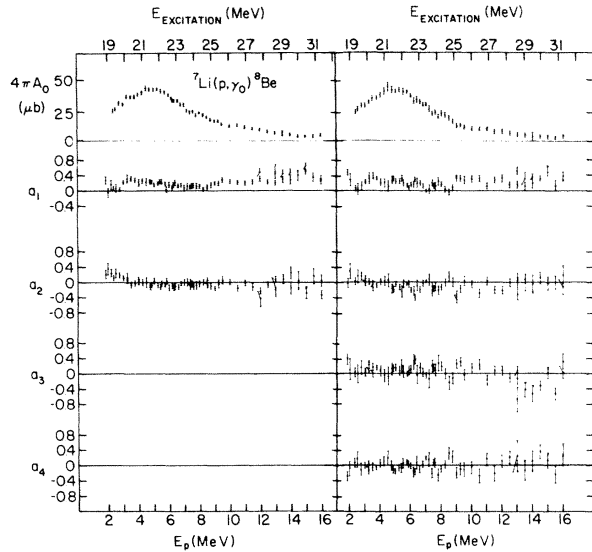


FIG. 6. Plot of the total cross section $4\pi A_0$ and the Legendre coefficients a_1 and a_2 (left side) and a_1 through a_4 (right side), obtained from the angular distribution fits, as a function of bombarding energy for the γ_0 transition.

result is significantly larger. The experimentally observed M1 strength for the $18.15 \rightarrow 2.9$ transition is much larger than can be explained simply, either by assuming a pure 1^+ , $T = 0$ state or by allowing an admixture from the 1^+ , $T = 1$ state at 17.6 MeV, in agreement with other evidence.¹⁴ A better theoretical value could only be obtained (see last column of Table I) by mixing in an additional $T = 1$ state at higher energies. The calculations of Barker¹⁶ predicted a 1^+ , $T = 1$ state at

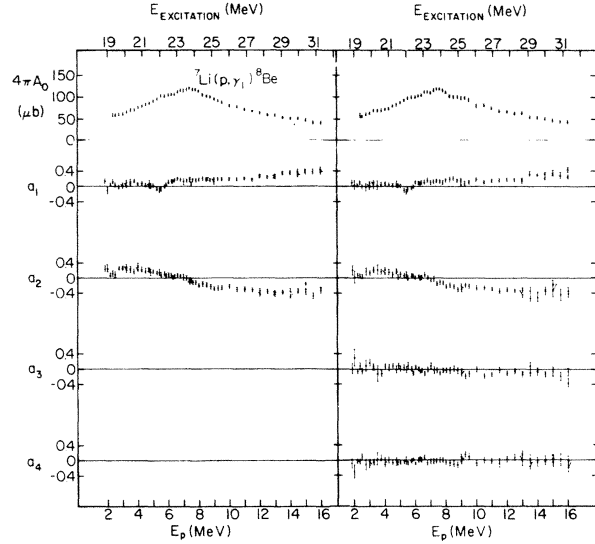


FIG. 7. Plot of the total cross section $4\pi A_0$ and the Legendre coefficients a_1 and a_2 (left side) and a_1 through a_4 (right side), obtained from the angular distribution fits, as a function of bombarding energy for the γ_1 transition.

19.4 MeV and a suitable parent state is known¹⁷ in ^8Li at 3.21 MeV excitation, corresponding to 20 MeV in ^8Be , with a width of about 1 MeV. Observation of this state directly in ^8Be has not yet been reported,¹⁸ but a $J = 1$ state seen in the (p, n) reaction at 19.4 MeV ($\Gamma = 750$ keV) is a possible candidate. The negative parity currently assigned to this state is based on circumstantial evidence only.^{17,19}

The level at $E_x = 19.06$ MeV has been

TABLE I. Gamma decay properties of states in ^8Be at 18.15 and 19.05 MeV.

Transition	Γ_γ (eV)			$\Lambda(M1)/(2J + 1)^a$		
	This exp. ^b	Other exps.	W. u. ^c	This exp.	Theor. ^d	Theor. ^e
18.15 \rightarrow 0.0	3.0	1.8 ^f	115	0.19	0.03	0.05
18.15 \rightarrow 2.9	3.8	3.6 ^f	70	0.07	0.004	0.09
19.06 \rightarrow 2.9	10.5	17.0 ^g	80	0.11		

^a $\Lambda(M1)$ is the reduced M1 width; J is the final-state spin.

^b $\Gamma_p = \Gamma$ is assumed.

^c W. u. is Weisskopf estimate for an M1 transition.

^d Reference 15.

^e With 5% mixture from a possible $(1^+, 1)$ state at 19.4 MeV, see text.

^f Reference 12.

^g Reference 13.

assigned $J^+ = 3^+$.¹⁹ This is consistent with its large γ_1 width and negligible γ_0 width. The observed γ_1 strength given in Table I then corresponds to a strong M1 decay for this mass region. The analysis of the angular distribution taken on top of this resonance introduces P_3 and P_4 Legendre polynomials into the fitting function (see data at $E_p = 2$ MeV in Fig. 7). This would indicate a strong E2 as well as an M1 width in the $3^+ \rightarrow 2^+$ transition, the P_4 term arising directly from E2 radiation,⁴ and the P_3 term from interference with the E1 background. The 3^+ state in ${}^8\text{Li}$ at 2.26 MeV is presumably the analog of this 3^+ level in ${}^8\text{Be}$.

B. The γ_0 giant resonance

The γ_0 giant resonance seen in Fig. 3 peaks at $E_x = 21.6$ MeV and has a peak cross section of approximately 2.7 $\mu\text{b}/\text{sr}$. Between $E_x = 18$ and 33 MeV, the cross section of the reaction ${}^8\text{Be}(\gamma, p_0){}^7\text{Li}$, obtained from these data by detailed balance, exhausts about 11% of the classical Thomas-Reiche-Kuhn sum rule:

$$\int_{18}^{33} \sigma(E) dE \approx 13 \pm 4 \text{ MeV mb} \\ \approx (0.11 \pm 0.03) 60 \frac{NZ}{A} \text{ MeV mb.}$$

Over a similar region of excitation in the giant E1 resonances of ${}^4\text{He}$, ${}^{12}\text{C}$ and ${}^{16}\text{O}$, the p_0 channels exhaust between 18 and 35% of the classical sum as seen in Table II. Thus, the (γ, p_0) strength in ${}^8\text{Be}$ is smaller than in the other 4N nuclei of the 1s and 1p shell.

We now attempt to understand the relative absorption cross sections in ${}^8\text{Be}$ and ${}^{12}\text{C}$ in the framework of the lp-lh model in its simplest, schematic form. We

assume that the collective dipole strength is given by the sum of all available lp-lh E1 transition strengths, which are thoroughly mixed so as to give the observed constant angular distributions (see below). We remark that in the usual microscopic p-h calculation the various p-h configurations are found to be concentrated at different excitation energies. It is further assumed that the ${}^8\text{Be}$ ground state is represented by the configuration $(s_{1/2})_{J=0}^4 (p_{3/2})_{J=0}^4$ and ${}^{12}\text{C}$ by $(s_{1/2})_{J=0}^4 2(p_{3/2})_{J=0}^4$. It is then straightforward to calculate the various p \rightarrow h transitions (computed in a harmonic oscillator well with $\hbar\omega = 41/A^{1/3}$ MeV) and their relative contribution in ${}^8\text{Be}$ and ${}^{12}\text{C}$ based on the statistical factors of the initial (hole) and final (particle) state (see Table III). Obviously the $p_{3/2}^{-1}d_{5/2}$ component dominates the absorption, although the other configurations make substantial contributions. After taking account of the factor $A^{1/3}$, one finds from Table III

$$B(E1, {}^8\text{Be})/B(E1, {}^{12}\text{C}) = 0.60.$$

This ratio can be related to the ratio of partial absorption cross sections R by using the relation $\int \sigma(\gamma, p_0) dE \propto E_\gamma^3 B(E1, \uparrow) (\Gamma_{p_0}/\Gamma)$ where E_γ is the peak γ -ray energy, Γ the total width, and $\Gamma_{p_0} = 2P\gamma_{p_0}^2$. One can now follow the model further by assuming for the proton reduced width

$$\gamma_{p_0}^2 = \frac{\sum_n c^2(n, p_{3/2}^{-1})}{\sum_{n,m} c^2(n, m^{-1})}$$

where the coefficients $c^2(n, m^{-1})$ refer

TABLE II. Properties of GDR in light 4N nuclei.

	Values on peak of GDR					$\langle a_2 \rangle$	$\int_{E_1}^{E_2} \sigma(\gamma, p_0) dE^a$	(% S.R.)
	E_p (MeV)	E_γ (MeV)	$\sigma(p, \gamma_0)$ (μb)	$\sigma(\gamma, p_0)$ (mb)	Γ_{cm} (MeV)			
${}^4\text{He}^b$	10.0	27.3	68	1.92	20	-0.98	21_{18}^{33}	35
${}^8\text{Be}^c$	5.0	21.6	33	2.05	5.3	-0.05	13_{18}^{33}	11
${}^{12}\text{C}^d$	7.3	22.6	137	12.2	3.5	-0.55	56_{16}^{29}	31
${}^{16}\text{O}^e$	10.8	22.2	177	12.7	4.2	-0.51	43_{12}^{29}	18

^a E_1 and E_2 are shown as subscripts and superscripts, respectively.

^b References 20 and 21.

^c Present work.

^d References 2 and 21.

^e Reference 22.

TABLE III. Relative contributions of lp-lh transitions to the electric dipole absorption in ^8Be and ^{12}C in a seniority scheme, all in relative units of $A^{1/3}$.

Configuration	$ \langle E1 \rangle ^2$	Relative contribution to $B(E1, \uparrow)$	
		^8Be	^{12}C
$(1s_{1/2})^{-1}(1p_{3/2})$	0.477	0.239	0
$(1s_{1/2})^{-1}(1p_{1/2})$	0.239	0.239	0.239
$(1p_{3/2})^{-1}(1d_{5/2})$	1.433	0.717	1.433
$(1p_{3/2})^{-1}(1d_{3/2})$	0.159	0.080	0.159
$(1p_{3/2})^{-1}(2s_{1/2})$	0.318	0.159	0.318
Total		1.434	2.15

to the wave-function coefficients for an n particle and an m hole (in the numerator $m = p_{3/2}$), and all coefficients are proportional to their associated E1 matrix elements listed in Table III. Using the parameters of Table II one obtains the ratio

$$R = \frac{\int \sigma(^8\text{Be})}{\int \sigma(^{12}\text{C})} = 0.28$$

before the proton penetrabilities P have been included. A rough estimate for d-wave penetrabilities at the peak energies in ^8Be and ^{12}C gives another reduction of about 0.5 for a square-well potential. With or without penetrabilities, the estimate for R agrees rather well with the observed value of 0.23. Thus the smaller strength observed in ^8Be , relative to ^{12}C , simply reflects the smaller number of $p_{3/2}$ particles in the ground state of ^8Be . The missing strength, of course, goes to excited states.

It is, of course, well known that multiple p-h components can be quite important in the GDR, the best example being the structure attributed to interference in the GDR of ^{16}O .²³ No such prominent structure is observed in either ^{12}C or ^8Be . This lack of structure could indicate that multiple p-h components lie well above the GDR in ^{12}C and ^8Be , in contrast to the "closed-shell" nucleus ^{16}O . Thus, the total width of the GDR in ^{12}C and ^8Be should arise mostly from particle escape with very little damping.

Finally, we note that no direct evidence for a static ground state deformation in ^8Be is apparent in the γ_0 excitation function. However, it is not clear how such deformation would express itself quantitatively in the GDR of such a light nucleus.

C. The γ_0 angular distributions

The characteristics of the γ_0 angular distribution can be seen in Fig. 6. The a_1 coefficient is positive with an average value between 0.1 and 0.4. Above $E_x = 24$ MeV, a_1 increases with increasing

excitation energy. A non-zero a_1 coefficient results from an interference between configurations of opposite parity. In this case, it may arise from the negative parity E1 giant resonance interfering with a positive parity E2 giant resonance located at a higher energy. This behavior is similar to that observed in other nuclei such as ^{12}C and ^{16}O .^{2,3,24}

The a_2 coefficient is virtually constant over the region above $E_x = 20$ MeV with an average value of about -0.05. A nearly constant a_2 coefficient is typical of the photoproton giant resonance and gives evidence for the fact that the GDR is dominated by a single collective state.²⁵ In fact, ^{12}C was among the first cases where this constancy of the a_2 coefficient was demonstrated. As can be seen in Table II, the absolute value for a_2 in ^8Be is much smaller than that in ^{12}C or ^{16}O , the latter values being more typical of the GDR. This difference will be discussed below.

As can be seen in Fig. 6, the a_3 coefficient is small, positive and quite constant throughout the giant resonance (up to about $E_x = 28$ MeV). This small value indicates a small amount of E2 radiation mixing in with the E1 radiation. However, above $E_x = 28$ MeV the a_3 coefficient becomes negative and larger in magnitude indicating a greater, and perhaps resonant, contribution from E2 strength located above the E1 resonance. However, the a_4 coefficient nowhere deviates significantly from zero, indicating that the E2 intensity is indeed very small compared to the E1 intensity, as expected from a comparison of the E2 and E1 sum rules.²⁶ No attempt will be made here to determine the E2 intensity quantitatively, since measurements with polarized protons are required to do this unambiguously.²⁷

If we are interested in determining only the E1 configuration of the giant resonance formed in the (γ, p_0) process, we may consider only the a_2 coefficients of the angular distribution and obtain, for capture by a $J^\pi = 3/2^-$ target nucleus,

$$\begin{aligned}
 a_2 = & 0.4(d_{3/2})^2 - 0.4(d_{5/2})^2 \\
 & + 0.6(d_{3/2})(d_{5/2}) \\
 & - [0.45(s_{1/2})(d_{3/2}) \\
 & - 1.34(s_{1/2})(d_{5/2})] \cos \delta \quad (2)
 \end{aligned}$$

where $s_{1/2} e^{i\phi_s}$, $d_{3/2} e^{i\phi_d}$ and $d_{5/2} e^{i\phi_s}$ are the complex amplitudes of the proton waves normalized to

$$(s_{1/2})^2 + (d_{3/2})^2 + (d_{5/2})^2 = 1 \quad (3)$$

and $\delta = \phi_s - \phi_d$. This expression for a_2 is identical to that obtained for the giant resonance in ^{12}C formed in $^{11}\text{B}(p, \gamma_0)^{12}\text{C}$.² In Eq. (2) it is assumed that the $d_{3/2}$ and $d_{5/2}$ amplitudes have the same phase ϕ_d . If we take for δ the difference between the Coulomb scattering phase shifts of s and d waves, then $\cos \delta$ depends on the nuclear radius and the incident proton energy. For $R = 1.2 A^{1/3}$ fm, one finds that $\cos \delta$ varies from about 1.0 at $E = 3.0$ MeV to about 0.5 at $E_p = 12$ MeV. If we set a_2

in Eq. (2) equal to its average experimental value of -0.05 , we find that the partial-wave solutions are allowed to have a continuous range of values. Also, because of the quadratic nature of the equations there are two independent solutions. These two solutions are plotted in Fig. 8 for $\cos \delta = 1.0$ and for $\cos \delta = 0.5$.

As expected, the small value of a_2 can be fitted by an almost pure $s_{1/2}$ wave ($s_{1/2}|s_{1/2}| \approx -1$ in Fig. 8). However, solutions which have large $d_{3/2}$ and/or $d_{5/2}$ amplitudes are also possible. If we consider only the $p_{3/2}$ -hole configuration in Table III, we obtain the solution: 75% $d_{5/2}^2$, 17% $s_{1/2}^2$ and 8% $d_{3/2}^2$, in terms of the normalization of Eq. (3). Although the $(p_{3/2})^{-1}(d_{3/2})$ contribution, in which the spin orientation is different in initial and final state, is normally small, it is comparable in strength to the $(p_{3/2})^{-1}(s_{1/2})$ transition which involves a node change. It is apparent from Fig. 8 that this solution is an allowed solution lying between the extreme possibilities. It is interesting that this solution, shown by the dots in Fig. 8, corresponds to a point where solutions I and II are practically degenerate with $\cos \theta = 0.70$. However, it must be emphasized that there is no experimental basis for selecting this or any other of the allowed solutions. Measurements with polarized protons would further limit the range of possibilities.

D. The γ_1 giant resonance

The giant resonance built upon the first excited state of ^8Be peaks at $E_x = 23.8$ MeV (Fig. 3). As can be seen from Fig. 7 the main γ_1 transition strength proceeds via $E1$ radiation and thus, the contributing states can only have $J^\pi = 1^-, 2^-$ and 3^- . However, if the coupling between the $E1$ excitation and the first excited state is weak, then one expects the γ_1 resonance to lie at an energy above the peak in the γ_0 resonance equal to the excitation of the first excited state ($E_x = 2.9$ MeV) with all spin states nearly degenerate. In fact, the experimental energy separation of the γ_0 and γ_1 resonances is 2.2 MeV.

The inverse reaction $^8\text{Be}^*(\gamma_1, p_0)^7\text{Li}$, obtained by detailed balance, exhausts about the same amount of the dipole sum rule as does the reaction $^8\text{Be}(\gamma_0, p_0)^7\text{Li}$. Thus, the much larger strength exhibited by the first excited state transition (Fig. 3) can be attributed to the statistical factor $2J + 1 = 5$ which appears when $B(E1, \uparrow)$ is changed to $B(E1, \downarrow)$. If the first excited state in ^8Be is loosely coupled to the dipole excitation, it is not unexpected that the reduced strengths for γ_0 and γ_1 are comparable. In addition, if the first excited state has rotational character then the internal wave functions should be similar for ^8Be and $^8\text{Be}^*$ and the same dipole state would be excited in each case.

The 90° yield for γ_1 shown in Fig. 3 exhibits some structure at $E_x \approx 21.4$ and

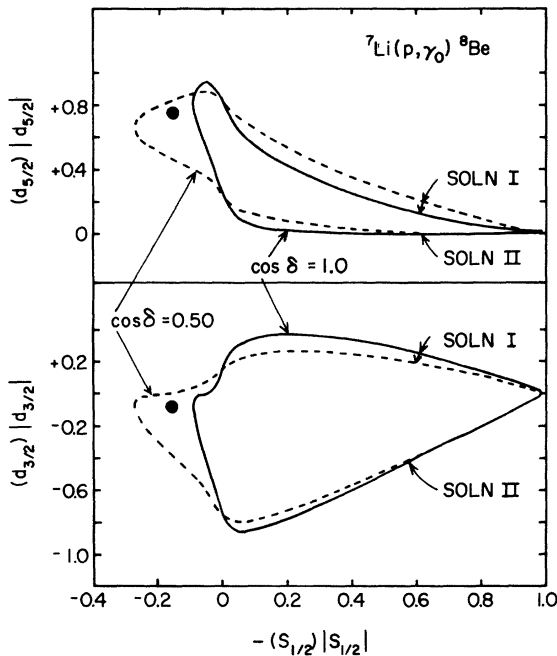


FIG. 8. Contour diagram of the relative $d_{5/2}^2$, $d_{3/2}^2$ and $s_{1/2}^2$ intensities in the proton capture reaction $^7\text{Li}(p, \gamma_0)^8\text{Be}$ which yield the observed a_2 coefficient ($a_2 = 0.05$). Curves are given for the two extreme relative phases δ between s and d waves and for the two branches corresponding to the two possible solutions. The configurations predicted by the schematic model (see text) are shown by the dots.

22.5 MeV superposed on the main GDR. The weaker structure at $E_x \approx 21.4$ MeV shows up more clearly in data taken at $\theta_\gamma = 0^\circ$. The structure at 22.5 MeV may be correlated with the structure seen in the γ_0 resonance.

E. The γ_1 angular distributions

The characteristics of the γ_1 angular distributions can be observed in Fig. 7. The a_1 coefficient is generally positive and increases with increasing excitation energy. The a_2 coefficient decreases with increasing energy, being positive at low energy, passing through zero in the region of the maximum yield, and becoming large and negative at higher energy. The a_3 coefficient is small but becomes definitely negative and increases in magnitude with increasing energy. Finally, the a_4 coefficient is small and consistent with zero throughout the energy range covered.

As in the case of γ_0 a broad giant quadrupole resonance built upon the first excited state can be invoked to explain the behavior of the a_1 and a_3 coefficients, but again the intensity of the resonance is not large enough to produce a significant a_4 coefficient.

The structure apparent in a_1 near $E_x = 22$ MeV is perhaps evidence for a positive parity state in this region. The only previously suggested states in ${}^8\text{Be}$ with positive parity in this energy region are at $E_x = 21.5$ MeV ($J^\pi = 3^+$, $\Gamma = 1.0$ MeV) and $E_x = 22.2$ MeV ($J^\pi = 2^+$, $\Gamma = 0.8$ MeV).¹⁸ The structure in the total yield in this excitation region also may be correlated with this fluctuation in the a_1 coefficient (see however Section III.D above).

As in the case of other giant resonances, the a_2 coefficient shows no significant structure throughout the GDR. This is all the more remarkable because of the increased complexity of the GDR with possible states of $J^\pi = 1^-, 2^-,$ and 3^- which allow a greater number of possible configurations. Because of this increased complexity, however, it does not seem useful to attempt to analyze the angular distributions in terms of the configurations.

IV. SUMMARY

The reactions ${}^7\text{Li}(p, \gamma_0){}^8\text{Be}$ and ${}^7\text{Li}(p, \gamma_1){}^8\text{Be}$ exhibit characteristic giant dipole resonances with little fine structure. The γ_0 giant resonance exhausts about 11% of the classical dipole sum rule, which is about half to a third of the typical value in the lp shell. The γ_0 angular distributions are nearly constant over the entire giant resonance region, an indication that a single state of mixed configuration dominates the region. A rather pure $(p_{3/2})^{-1}(d_{5/2})$ configuration with small admixtures of the $(p_{3/2})^{-1}(s_{1/2})$ and $(p_{3/2})^{-1}(d_{3/2})$ configurations can explain the nearly isotropic ($a_2 = -0.05$) and constant angular distributions. This result, as

well as the observed absorption strength of ${}^8\text{Be}$ relative to ${}^{12}\text{C}$ is semi-quantitatively explained by a schematic lp-lh model of the GDR in which the various lp-lh configurations are thoroughly mixed to give the observed constant angular distributions.

No definite evidence is obtained regarding the possible deformation of ${}^8\text{Be}$ relative to ${}^{12}\text{C}$. The γ_0 and γ_1 giant resonances in ${}^8\text{Be}$ are compared with the γ_0 resonances in ${}^4\text{He}$ and ${}^{12}\text{C}$ in Fig. 9. Also in this figure, there is no convincing evidence that the GDR of ${}^8\text{Be}$ is similar to that of ${}^4\text{He}$, which might indicate α clustering in ${}^8\text{Be}$. Although the GDR of ${}^8\text{Be}$ is rather featureless it is considerably more compact than the GDR of ${}^4\text{He}$.

The γ_1 giant resonance lies above the γ_0 resonance by about 2.2 MeV, which is approximately equal to the excitation of the first excited state. Note the comparison of the two resonances in Fig. 9 when the γ_1 resonance has been shifted down by 2.9 MeV. The resonance also exhausts

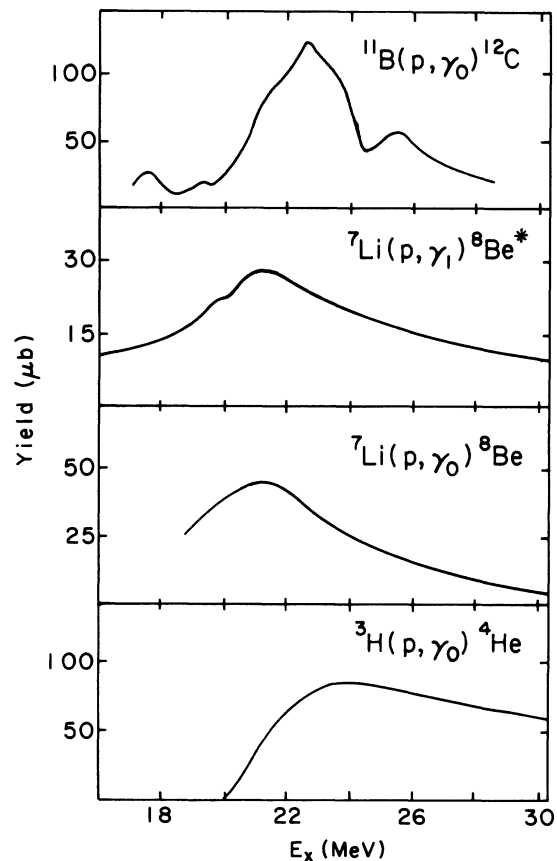


FIG. 9. A comparison of giant resonances in ${}^{12}\text{C}$, ${}^8\text{Be}$, and ${}^4\text{He}$ as observed with the (p_0, γ) reaction. For comparison purpose the γ_1 resonance has been shifted down by 2.9 MeV, the excitation of the first excited state.

about 10% of the dipole sum rule. That the (γ_0, p_0) and (γ_1, p_0) strengths are comparable is plausible if the dipole excitation is weakly coupled to the first excited "rotational" state of ^8Be . A

detailed analysis of the γ_1 resonance is not warranted at present, but it appears that it is also dominated by a single E1 configuration.

- [†]Supported in part by the National Science Foundation.
- *Present address: Department of Physics, San Francisco State University, San Francisco, California 94132.
- [‡]Present address: Department of Physics, State University of New York, Stony Brook, New York 11794.
- [§]Present address: Sektion Physik der Universität München, München, Germany.
- ¹E. Hayward, *Revs. Mod. Phys.* **35**, 324 (1963); in *Nuclear Structure and Electromagnetic Interactions*, edited by N. MacDonald (Plenum, New York, 1965), p. 141.
- ²R. G. Allas, S. S. Hanna, L. Meyer-Schützmeister, and R. E. Segel, *Nucl. Phys.* **58**, 122 (1964); W. A. Lockstet and W. E. Stephens, *Phys. Rev.* **141**, 1002 (1966).
- ³N. W. Tanner, G. C. Thomas, and E. D. Earle, *Nucl. Phys.* **52**, 29 (1964); R. L. Bramblett, J. T. Caldwell, R. R. Harvey, and S. C. Fultz, *Phys. Rev.* **133**, B869 (1964).
- ⁴N. Vinh-Mau and G. E. Brown, *Nucl. Phys.* **29**, 89 (1962).
- ⁵V. Gillet and N. Vinh-Mau, *Nucl. Phys.* **54**, 321 (1964).
- ⁶D. H. Wilkinson, *Physica* **22**, 1039 (1956); *Ann. Rev. Nucl. Sci.* **9**, 1 (1959).
- ⁷G. E. Brown and M. Bolsterli, *Phys. Rev. Lett.* **3**, 472 (1959).
- ⁸D. S. Gemmell, A. H. Morton, and E. W. Titterton, *Nucl. Phys.* **10**, 33 (1959).
- ⁹I. V. Mitchell and R. B. Taylor, *Nucl. Phys.* **44**, 664 (1963); R. R. Perry, B. Mainsbridge, and J. Richards, *Nucl. Phys.* **45**, 586 (1963).
- ¹⁰E. G. Fuller and M. S. Weiss, *Phys. Rev.* **112**, 560 (1958); R. L. Bramblett, J. T. Caldwell, G. F. Auchampaugh, and S. C. Fultz, *Phys. Rev.* **129**, 2723 (1963).
- ¹¹M. Suffert, W. Feldman, J. Mahieux, and S. S. Hanna, *Nucl. Instr. and Meth.* **63**, 1 (1968).
- ¹²A. A. Kraus, *Phys. Rev.* **93**, 1308 (1954); B. Mainsbridge, *Australian J. Phys.* **13**, 204 (1960); see also Reference 14.
- ¹³L. Nilsson and I. Bergvist, *Arkiv Fysik* **35**, 411 (1967).
- ¹⁴F. Paul, D. Kohler, and K. A. Snover, *Phys. Rev.* **173**, 919 (1968).
- ¹⁵S. Cohen and D. Kurath, *Nucl. Phys.* **73**, 29 (1965).
- ¹⁶F. C. Barker, *Nucl. Phys.* **A83**, 418 (1966).
- ¹⁷J. M. Freeman, A. M. Lane, and B. Rose, *Phil. Mag.* **46**, 17 (1955); G. Presser and R. Bass, *Nucl. Phys.* **A182**, 321 (1972).
- ¹⁸F. Ajzenberg-Selove and T. Lauritsen, *Nucl. Phys.* **A227**, 1 (1974).
- ¹⁹L. Brown, E. Steiner, L. G. Arnold, and R. G. Seyler, *Nucl. Phys.* **A206**, 353 (1973).
- ²⁰W. E. Meyerhof, M. Suffert, and W. Feldman, *Nucl. Phys.* **A148**, 211 (1970).
- ²¹S. S. Hanna, in *International Conference on Photoneuclear Reactions and Applications*, Asilomar, 1973, edited by B. L. Berman (Lawrence Livermore Laboratory, Livermore, 1973) Vol. I, p. 417.
- ²²W. J. O'Connell, Stanford University, Ph.D. thesis, 1969.
- ²³V. Gillet, M. A. Melkanoff, and J. Raynal, *Nucl. Phys.* **A97**, 631 (1967).
- ²⁴D. E. Frederick, R. J. J. Stewart, and R. G. Morrison, *Phys. Rev.* **186**, 992 (1969); D. E. Frederick and S. A. Daniel, *Phys. Rev.* **176**, 1177 (1968).
- ²⁵R. G. Allas, S. S. Hanna, L. Meyer-Schützmeister, R. E. Segel, P. P. Singh, and Z. Vager, *Phys. Rev. Lett.* **13**, 628 (1964).
- ²⁶E. Kuhlmann, E. Ventura, J. R. Calarco, D. G. Mavis, and S. S. Hanna, *Phys. Rev. C*, **11**, 1525 (1975).
- ²⁷S. S. Hanna, H. F. Glavish, R. Avida, J. R. Calarco, E. Kuhlmann, and R. LaCanna, *Phys. Rev. Lett.* **32**, 114 (1974).